

A comparative study of Corrosion in an Aluminium alloy and mild steel using acoustic emission and microscopic techniques

A.M. Siddiqui, A. Abdu, A. Mahen, A.H. Choudhury
School Of Engineering, The Robert Gordon University,
Aberdeen, Scotland, U.K.
a.siddiqui@rgu.ac.uk

The study of corrosion needs no justification, as the cost of corrosion through the degradation of the metal or metal alloy and the consequences of corrosion are very high. Corrosion causes a terrible waste of natural resources, which in turn may cause all type of ecological damage through the product formed by the corrosion process.

In the oil and gas industry the major cause of most structure or component failures is the corrosion. Industry is constantly battling corrosion related issues such as pipeline leakage, structure or equipment failure. Failure on an offshore installation can be very costly due to loss in production, hazard to operators, environment and in some cases leading to total loss of installation like the Piper Alpha disaster [1].

In the aviation industry as the number of older aircrafts operating in the sky is increasing, so is the concern of the safety of the aircrafts and their users due to corrosion. The major form of failure for the older aircraft is corrosion fatigue. The aircrafts are subjected not only to cyclic service loading, but also to impact of sand, rain, an environment which is increasingly becoming polluted, (increasing content of acid, alkali and salts) and mechanical wear leading to corrosion fatigue.

Corrosion prevention or mitigation is an on going task, which never ends. One important aspect of corrosion control or prevention is corrosion monitoring.

The major functions of corrosion monitoring are:

- i. Diagnosis of corrosion problems
- ii. Identification of active corrosion sites
- iii. Monitoring the state of corrosion control methods (cathodic protection, inhibitors etc.)
- iv. Advanced warning of system upsets leading to corrosion damage
- v. Determination of inspection or maintenance schedules
- vi. Estimation of service life span of a structure.

The detection, characterization and quantification of corrosion damage cannot be relied on a single technique whether it may be electrochemical, electrical, analytical, and or NDT techniques including AE. No single technique is either suitable or ideal for monitoring all forms of corrosion.

On going research work on corrosion monitoring in the Robert Gordon University using AE is

to develop a database or a case-based strategy to predict the severity of corrosion under specific environmental conditions. This paper, based on student projects carried under the supervision [2], aims to compare the effect of two types of corrosive environments on the strength of an aluminium alloy and two kind of mild steels using acoustic emission, scanning electron microscope and atomic force microscopy. Microscopic investigation, evaluation of test results and unsupervised classification of the recorded AE waveforms for the reference and corroded samples clearly demonstrate the dependence of AE activity on the nature and type of corrosion and applied load.

Design and Methodology

Chemical Composition of test samples

The 3 different kinds of materials used in this study were:

- ☀ Mild Steel EN1A (Bright BS 970 230M07 ENDS BLACK)
- ☀ Mild Steel EN3B (Bright BS 970 080A15 ENDS BLACK)
- ☀ Aluminium (Alloy and Temper 6082-T6)

Their mineral composition is given in Table 1

Material EN3B BRIGHT BS 970 080A15

| C | Si | Mn | S | P | Pb | Ni | Cr | Mo | Cu | Al | V |
|-------|-------|-------|-------|-------|-------|-------|-------|-------|-------|-------|-------|
| 0.155 | 0.250 | 0.820 | 0.027 | 0.008 | 0.000 | 0.080 | 0.090 | 0.010 | 0.120 | 0.005 | 0.000 |
| | Cb | Sn | Fe | Mg | Zn | Ti | Se | Nb | Co | | |
| | 0.000 | 0.006 | 0.000 | 0.000 | 0.000 | 0.000 | 0.000 | 0.000 | 0.000 | | |

Material EN1A BRIGHT BS 970 230M07

| C | Si | Mn | S | P | Pb | Ni | Cr | Mo | Cu | Al | V |
|-------|-------|-------|-------|-------|-------|-------|-------|-------|-------|-------|-------|
| 0.090 | 0.015 | 1.130 | 0.267 | 0.056 | 0.000 | 0.000 | 0.000 | 0.000 | 0.000 | 0.000 | 0.000 |
| | Cb | Sn | Fe | Mg | Zn | Ti | Se | Nb | Co | | |
| | 0.000 | 0.000 | 0.000 | 0.000 | 0.000 | 0.000 | 0.000 | 0.000 | 0.000 | | |

Material Aluminium Alloy and Temper 6082-T6

| C | Si | Mn | S | P | Pb | Ni | Cr | Mo | Cu | Al | V |
|-------|-------|-------|-------|-------|-------|-------|-------|-------|-------|-------|-------|
| 0.000 | 0.980 | 0.533 | 0.000 | 0.000 | 0.001 | 0.000 | 0.005 | 0.000 | 0.030 | 0.000 | 0.009 |
| Zr | Cb | Sn | Fe | Mg | Zn | Ti | Se | Nb | Co | Bi | |
| 0.000 | 0.000 | 0.000 | 0.210 | 0.670 | 0.002 | 0.006 | 0.000 | 0.000 | 0.000 | 0.000 | |

Table 1 the mineral composition of the test samples

The specimens selected for corrosion tests were placed in two environmental chambers. For exposing the samples to humid and marine environments, the samples involved in each category were placed in a chamber where the temperature of 3% salt water and the environment was maintained at 60°C with relative humidity of 95%. The only difference between the marine and humid environment was that the samples in the marine category were submerged in a tray containing 3% salt water. The specimens for producing corrosion in the humid environment were only exposed to salt spray within the chamber itself. This was how the specimens were simulated as per the actual offshore structures condition in the sea. A typical sketch of the corrosion chamber for corroding the Aluminium specimens is shown in Figure (1) (Mild Steels in a separate similar chamber)

The duration of exposure of the specimens to accelerated corrosion was 54 days or 1296 hours.

The Test

The test parameters and procedures were established to simulate the loading condition of the offshore platform. Examples of loading conditions include wind loading, wave impact and tide etc.

The 3 different types of test conducted on the corroded and reference specimens were: -

- Tensile load test
- 3 point bending test
- 3 point fatigue cyclic test

The Instron model 1195 (2511 - 319) loading frame was used for tensile tests. The output of the load cell signal amplifier (10volt/100kN) was connected to one of the parametric inputs of the Vallen AMSY4 AE system. The speed of the crosshead was set to 10 mm/min for all tests. Basically all tests were carried out at room temperature of approximately between 15° - 20°C and with a relative humidity of 50%.

The samples after removing from the respective corrosive environment were cleaned, dried and in some cases corroded flakes were removed in order to enhance the detection quality of the Acoustic Emission during tests.

Two SE150kHz transducers were mounted on the surface of the specimen to record AE activity during the tensile loading.

Flexural and 3-Point Bending fatigue tests were carried out on Instron model 8500 Fatigue testing Machine. Figure 2a shows the Instron 8500 machine used for 3 point bending load test. The specimen was placed, by offsetting the notch of the specimen for about 10mm towards the right from the centre

roller. Two SE150kHz probes were attached to the specimen. The distance between the centres of the probes was 215 mm as shown in Figure2b

The Instron 8500 machine was set to load the specimens at a constant strain rate of 0.6 millimetres per minute (mm/m) and the AE activity was monitored. During fatigue test a cyclic load of 5kN was maintained by oscillating the loading frame at 2.5Hz between a minimum of 1kN and a maximum of 6kN. The behaviour of the specimen subjected to corrosion condition was analysed using acoustic emission and microscopic techniques. The recording of AE events was carried on until the loaded specimen indicated severe damage or fracture (cracks associated with high energy emissions).

Significance of the testing procedures

The position of centre load point is significant in three-point bending test arrangement. Basically the bending point curvature is a maximum at the centre roller position and not at the tip of the notch. The centre load offset produces two unequal moments (Force x arm length) in the specimen causing more damage and AE activity in the longer than the shorter arm.

The various acoustic emission signal parameters and waveforms recorded during static and cyclic stress applied to the specimens to identify sudden changes in the activity that might be an indication of initiation of new cracks and or their growth would include extraneous noise from roller friction etc. The eccentric load test procedure was significant in order to relate AE activity without interference from the central roller friction noise, to the size of a defect such as a sudden initiation or propagation of a crack and to determine the remaining safe life of the structure.

AFM (Atomic Force Microscope)

Some of the corroded samples were sectioned to compare the nature and severity of corrosion on surface and deformation in the fractured region using Atomic Force microscopy and scanning electron microscopic techniques

The atomic force microscope (AFM) is one of several types of scanned-proximity microscopes. These microscopes work by measuring a local property-such as force, height, magnetism or electric field- with a probe or a sharp tip placed very close to a sample. AFM operates by measuring forces between the tip and the sample. In the contact mode when the tip to sample distance is in the order of 0.3nm the force is repulsive and increases steeply with decreasing distance.

In principle, AFM resembles the record player as well as the stylus profilometer. However, AFM incorporates a number of refinements that enable it to achieve atomic-scale resolution:

- Sensitive detection
- Flexible cantilevers
- Sharp tips
- High resolution tip-sample positioning
- Force feedback

AFM results for marine corrosion

The diagram in Figure (3a) shows a 3D view of a section of the specimen covered uniformly with hills and valleys across the corroded specimen. The valleys are created by the transformation of Fe during the oxidation-reduction process. These sites are vacancies left by the displaced Fe atoms from the original corrosion free sites. These displaced atoms are oxidised (rust) and are deposited close by (hills).

A typical magnified corroded region is shown in Figure (3b)

AFM results for humid corrosion

The scattered bumpy surface appearance (Rust-FeOH₃) in Figure (4a) is due to relatively non-uniform corrosion film produced as a result of exposure of the specimen to humid environment.

The estimated size of a pit in the zoomed photograph, Figure (4b) is approximately 0.616nm much larger than atomic size (0.1 – 0.2nm), which suggests disruption of atomic structure at the pit.

AFM studies reported in this paper are limited to mild steel. Corrosion films formed on aluminium alloy have finer structure and are entirely different from the rust formed on steel. The results of AFM measurement carried out on the corroded aluminium specimen will be reported elsewhere.

Scanning electron micrographs of some corroded aluminium and mild steel samples fractured under tensile and cyclic loads are given in Figure (5).

The SEM micrograph of fractured section in aluminium shows inter-granular crack and in the case of steel in a similar fractured section regions of plastic flow can be seen. There are clearly wide differences in the microstructure of the corroded EN1A and EN3B samples.

The AFM and SEM results show a similar trend in microscopic surface changes in the specimens investigated as a result of exposure to humid and marine environments. The corroded film in the steel appears to be a build up of filliform corrosion.

ACOUSTIC EMISSION

A typical set of AE signal parameters recorded during various types of tests for the reference and corroded (marine and humid environment) samples are given. A comparison of AE results was carried out to investigate the effect of environment and loading condition on the strength and toughness of the materials.

Figure (6a) shows the effect of central roller offset. It is apparent that the recorded AE activity is relatively higher in the longer arm and at the notch location (13cm). Most of the events occurring in the region of the notch are high peak amplitude; low-rise time and longer duration indicating severity of damage i.e. crack initiation or growth.

The top row of multi plot in figure (7) shows the 3-point bend load history (constant strain rate of 0.6mm / min) on aluminium samples to fracture. For comparison purpose the AE peak distribution for equal time of 1600s is shown in the bottom row. It is apparent from the plots that humid environment induces more brittleness than the marine environment and also produces more energetic (high peak amplitude) signals. A large number of these high peak amplitude signals have longer duration, shorter rise time and are located in the notch region of the specimens.

Three point bending cyclic (fatigue) test

The AE activity recorded during the fatigue tests of the reference and corroded samples is shown in figure (8). For the purpose of comparison of fatigue behaviour of the samples tested, same set up for the display and analysis of the signal parameter was used. The top row in the multi plot shows peak amplitude ~ duration versus location and peak amplitude ~ rise time distribution versus test time. It can be seen that AE activity is higher in the longer arm and in the vicinity of notch region. Most of the signals in the notch region have longer event duration associated with low-rise time and relatively higher peak amplitude. It is evident that majority of these events are related to the crack initiation, growth and propagation.

The multi plot in the bottom row shows the event distribution history and recorded signal waveform.

The samples corroded in the humid and marine environment indicate additional events throughout the specimen as a result of corrosion product separating from the parent metal surface during fatigue loading. However these events have distinctly shorter event duration and lower value of peak amplitudes.

TENSILE TEST

The results of tensile tests carried out on aluminium reference and corroded samples are shown in figure (9).

Reference sample

The results obtained for the reference sample show that most events were of low duration and low peak amplitudes. These events occurred in the linear elastic region well below the yield point of aluminium and were mainly by the micro indentation of the grips holding the specimen. In the ductile region, just before the sample fractured, a number of high peak amplitudes and higher duration events were recorded. These events occurred during the necking and micro cracking of the specimen.

Humid sample

The number of events recorded in the elastic and ductile regions was more compared to the reference sample. It is apparent that the corrosive environment, which led to generate additional AE signals before the final fracture, influenced the specimen.

Marine sample

The AE activities recorded were highest for Marine sample compared to both humid and reference samples. In the linear-elastic region the AE activity was similar to the reference sample but increased much near the yield point and in the ductile region. The specimen was weakened by the corrosion attack and produced higher rate of emission events and activities.

AE SOURCE CHARACTERISATION

The waveforms recorded during all three types of tests on both aluminium and mild steel materials were analysed using unsupervised classification in order to discriminate between various events relating to deformation, separation of corrosion product, roller or grip friction and other sources occurring in the specimen under stress.

Typical sets of unsupervised classification, feature extraction and clustering results are shown in Figure (9). The circles were grouped as cluster 1 and belong to high peak amplitude, larger event

duration signals, which are the characteristics of crack initiation, growth and propagation in the samples under stress. In the reference sample Figure (9c) the clusters 2, 3 and 4 either have fewer group members or missing.

Figure (10a) shows the results of unsupervised classification of waveform data of a corroded (humid) EN3B steel sample. The group of waveforms representing cluster 1 are mostly associated with fatigue crack initiation and its growth as these signals belong to high amplitude, higher event duration and shorter rise time. Figure (10b) is a feature ~feature plot obtained by the application of the hc3B classification to EN1A corroded (marine) sample.

Typical sets of AE waveform data recorded during fatigue test were analysed using unsupervised classification. The population of 6 clusters representative of various sources of emission are shown in the histograms in Figure (11). The knowledge gained in this study has provided enough confidence to build a supervised classifier for future attempts to build a database for corrosion monitoring (assessment, control and prevention) using case based reasoning strategy.

The results of unsupervised classification applied to aluminium and steel respectively for 3 test modes are shown in the histograms in Figure (12).

CASE BASE REASONING AND CORROSION EMISSION MONITORING USING AE

Corrosion monitoring in a diverse branch of industry can be in real time, on-line or off-line (laboratory measurement). Acoustic emission has the potential to be applied to diverse industrial fields and can be real-time, on-line or off-line situations. It can provide information of active sites, their location, time, severity and changes in the rate of corrosion. Many commercial AE neural networks based or expert systems can not cope with the diversity of corrosion factors such as geometry of the system and components, process conditions, material of construction, type of environment and external factors. Thus, there is a need for a case based reasoning approach to this problem. This requires data based management of various corrosion cases relating to several diverse factors and data mining approach to a particular situation.

The CBR Cycle as shown in Figure (13) consists of a database containing AE and various complementary data from corrosion problems. When a new corrosion problem arises the CBR tool looks for similar case and adapts a solution. If the problem is new the operator intervenes to facilitate

a solution and updates the database for retention and future applications. A sketch of CBR cycle is shown in Figure (13).

It is planned to use the laboratory based AE corrosion monitoring data to run on the AIAI CBR Shell (Artificial _Intelligence_ Applications Institute), a generic tool which performs classification based on case comparison [3]. This work is in progress and will be reported elsewhere.

The results of microscopic studies have revealed that humid environment is more aggressive to both the mild steel and aluminium alloy which is in line with previous investigation on 7019 series aluminium alloy [4].

The AE monitoring data and its analysis in time and frequency domain has shown that it is possible to discriminate between various AE sources, to isolate corrosion related activity from other fracture sources. The experience gained in source characterisation is valuable and is used to build a supervised classification of the data.

In conclusion, through the work presented in this paper it is possible to predict the trend in which the corrosion in steel and aluminium alloy would occur. Further research in the field of corrosion monitoring will require more diverse data to build a database for further evaluation using case base reasoning methodology.

Reference:

- [1] Alexander, D.A, The Piper Oil rig disaster, International handbook of traumatic stress syndromes, pp 461-470, 1993, Plenum Press.
- [2] Dr A.M. Siddiqui, school of engineering, Robert Gordon University, Aberdeen.
- [3] AIAI CBR Shell, Artificial Intelligence Application Institute, Robert Gordon University, Aberdeen.
- [4] B. Knowlton, A.M. Siddiqui & S.Jihan, British Corrosion Journal, 3050 vol. 32 no 4, March 1998.

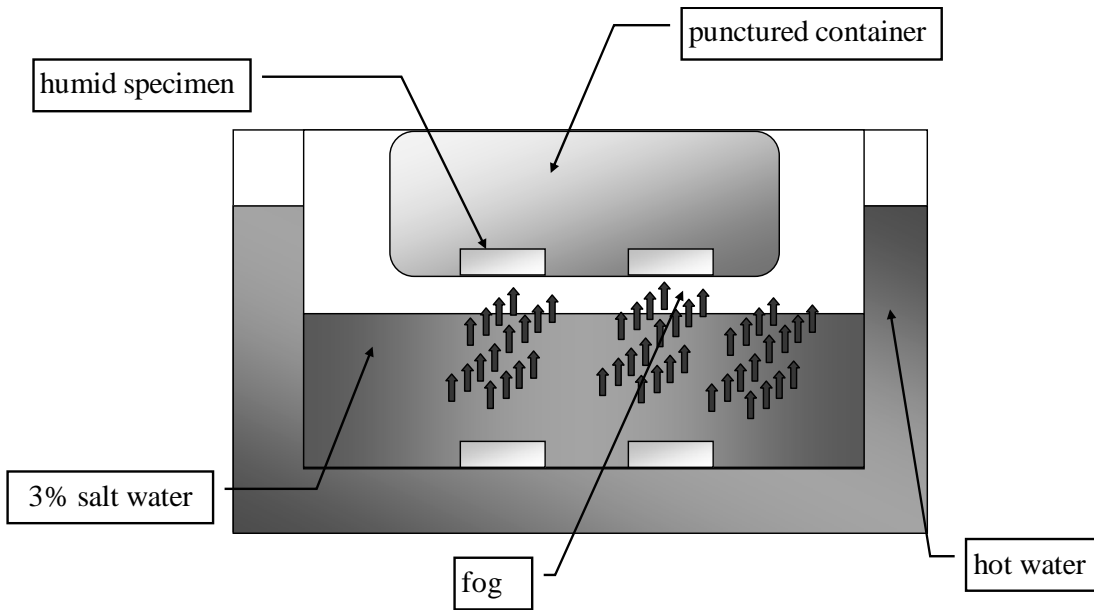


Figure (1). Corrosion Chamber

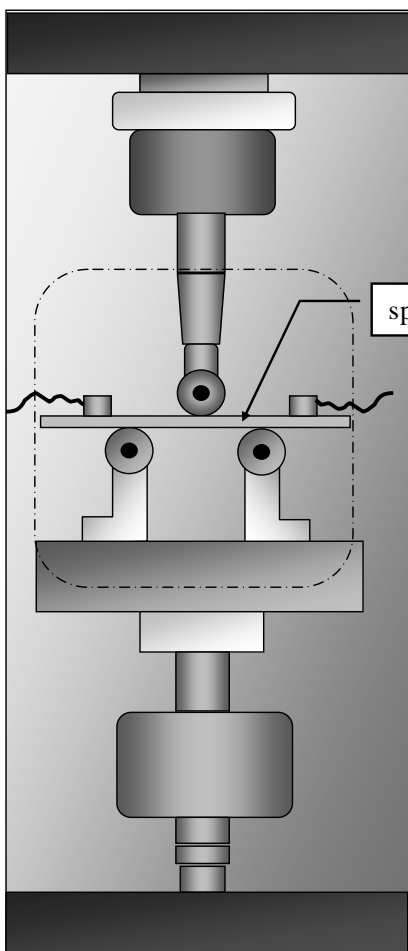


Figure (2a) Three Point bending test

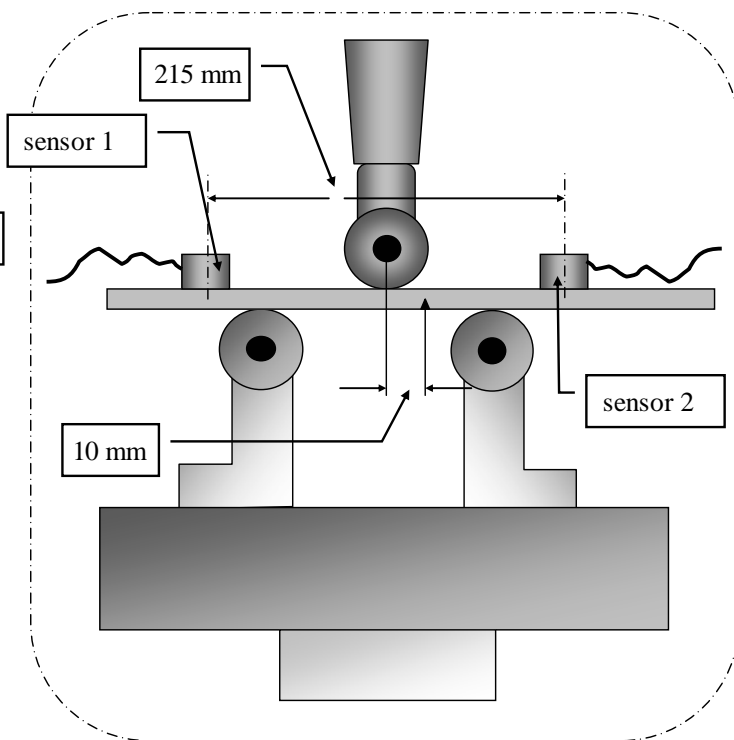


Figure 2b Eccentric load and position of Sensors

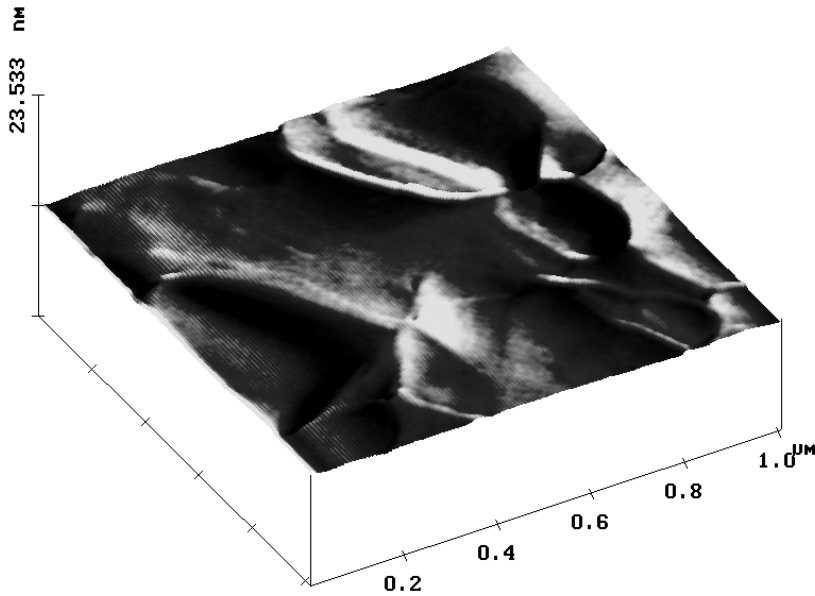


Figure (3a).

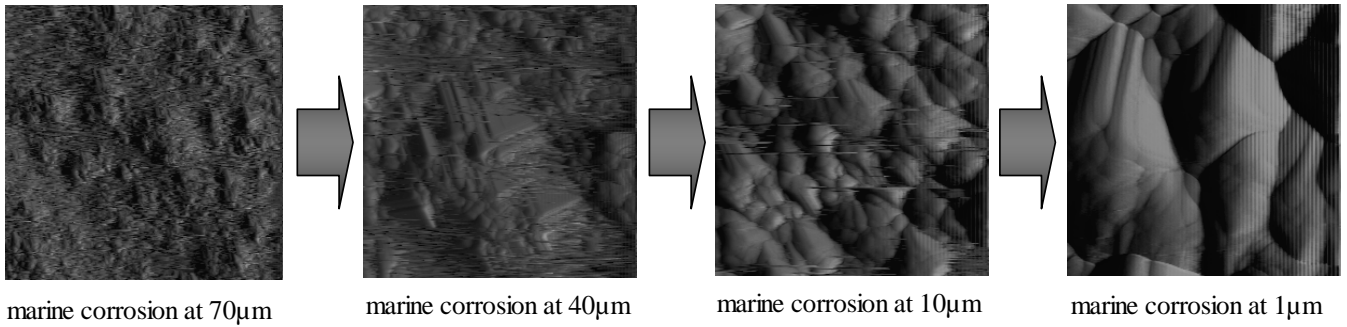
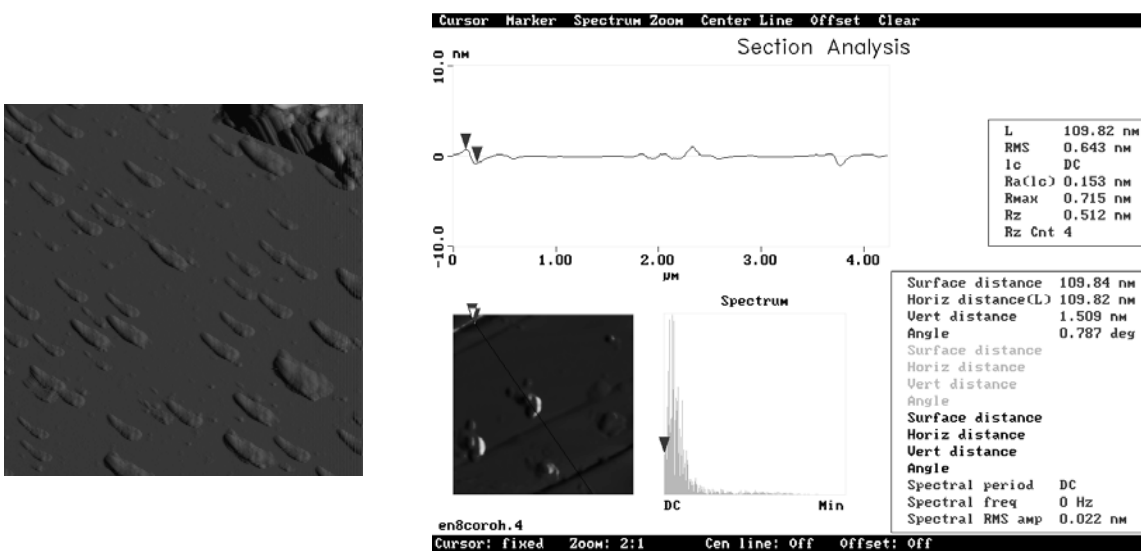
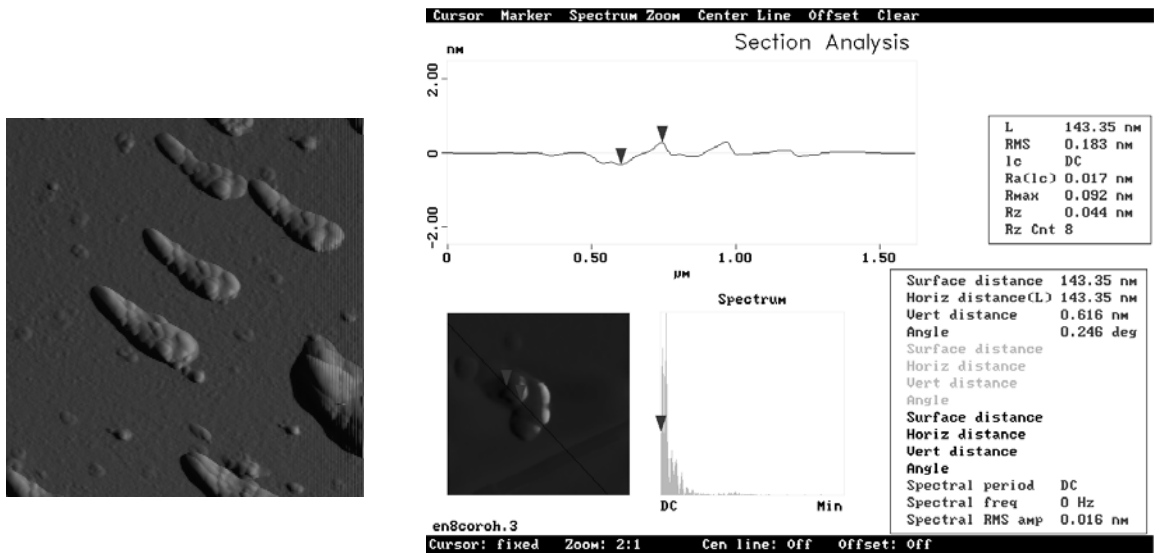


Figure (3b).

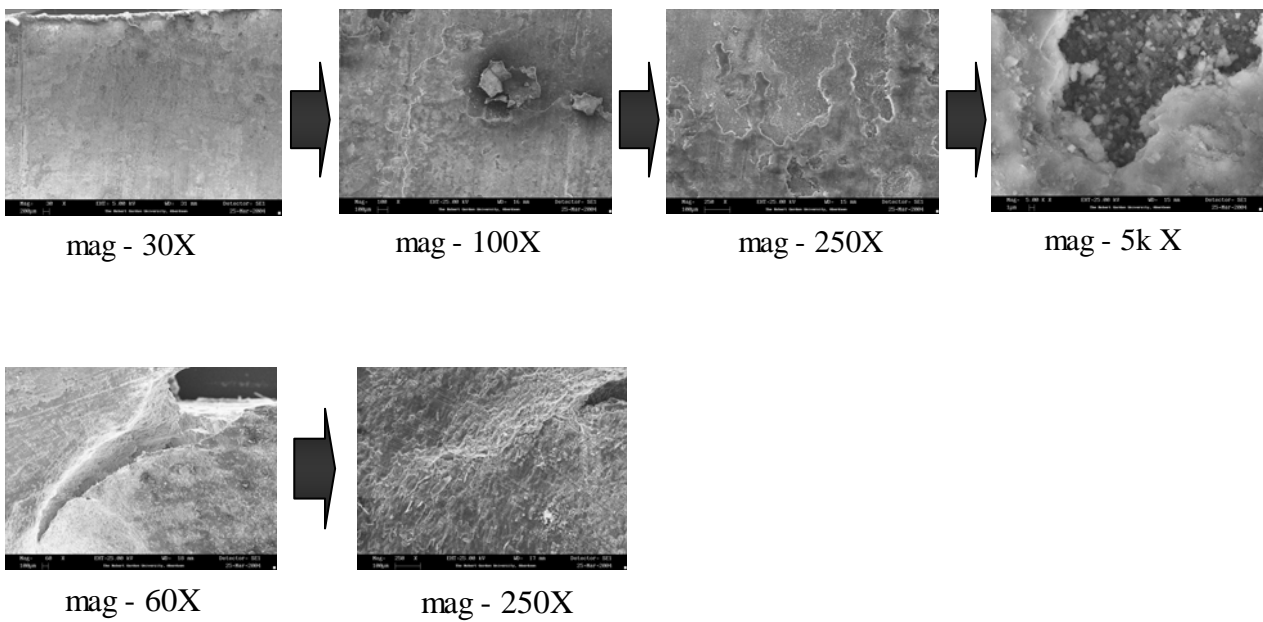


- Humid corrosion at 50 μ m Figure (4a)



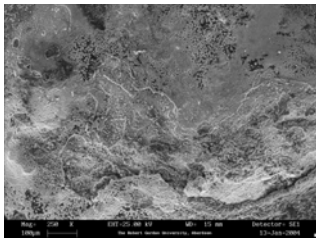
- Humid corrosion at 10μm Figure (4b)

Figure (5)
Aluminium

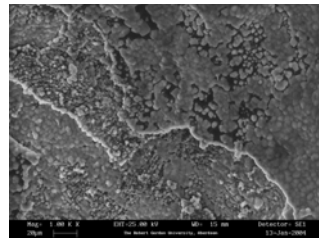


Steel

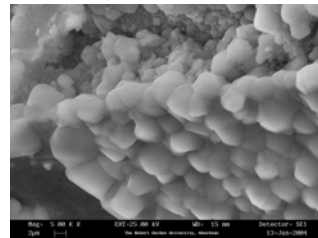
EN1A



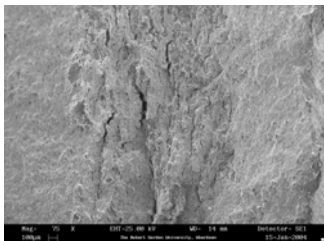
mag - 250X



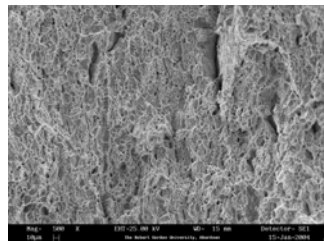
mag - 1 k X



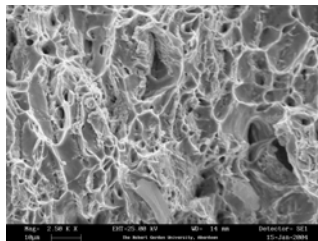
mag - 5 k X



mag - 75X

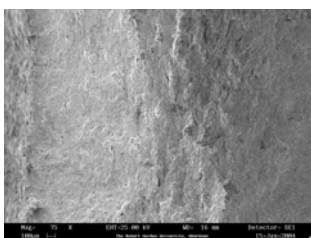


mag - 500X

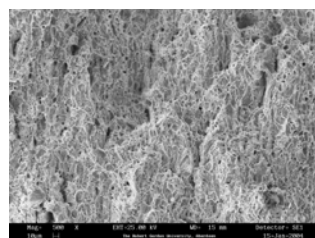


mag - 2.5k X

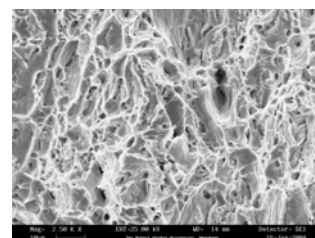
EN3B



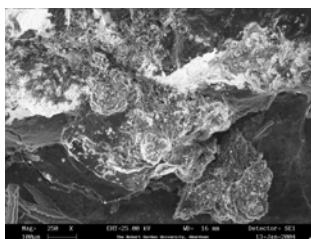
mag 75 X



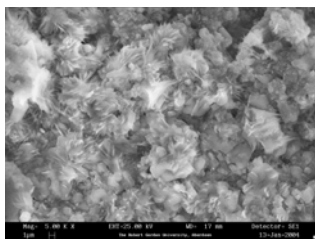
mag 500 X



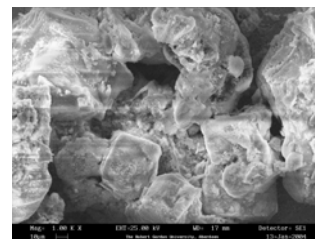
mag 2.5K X



mag 250 X



mag 5K X



mag 1K X

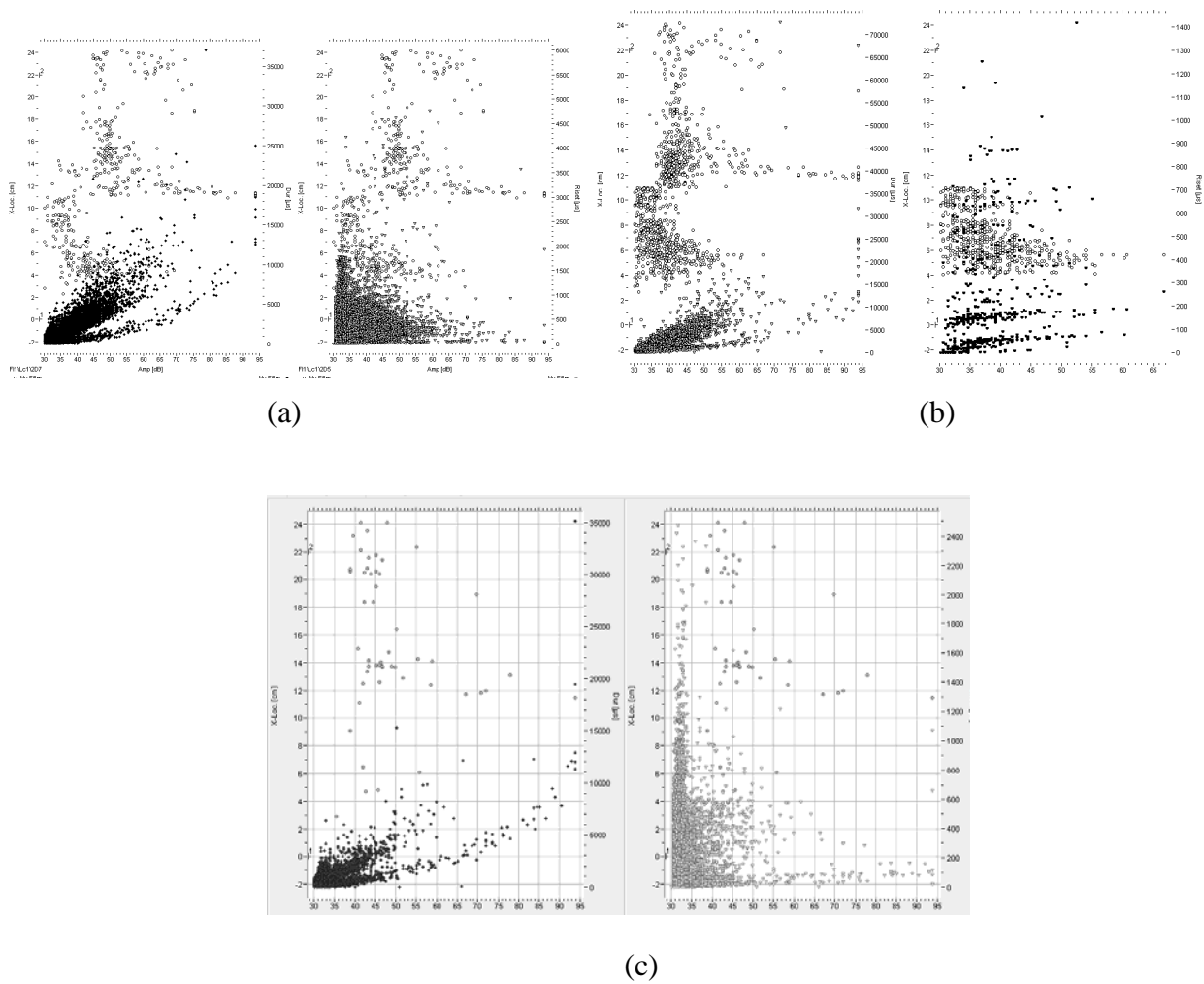


Figure (6) Flexural test on Al sample: Location, rise time/duration~ peak amplitude

(a) Reference (b) Humid corrosion and (c) Marine corrosion

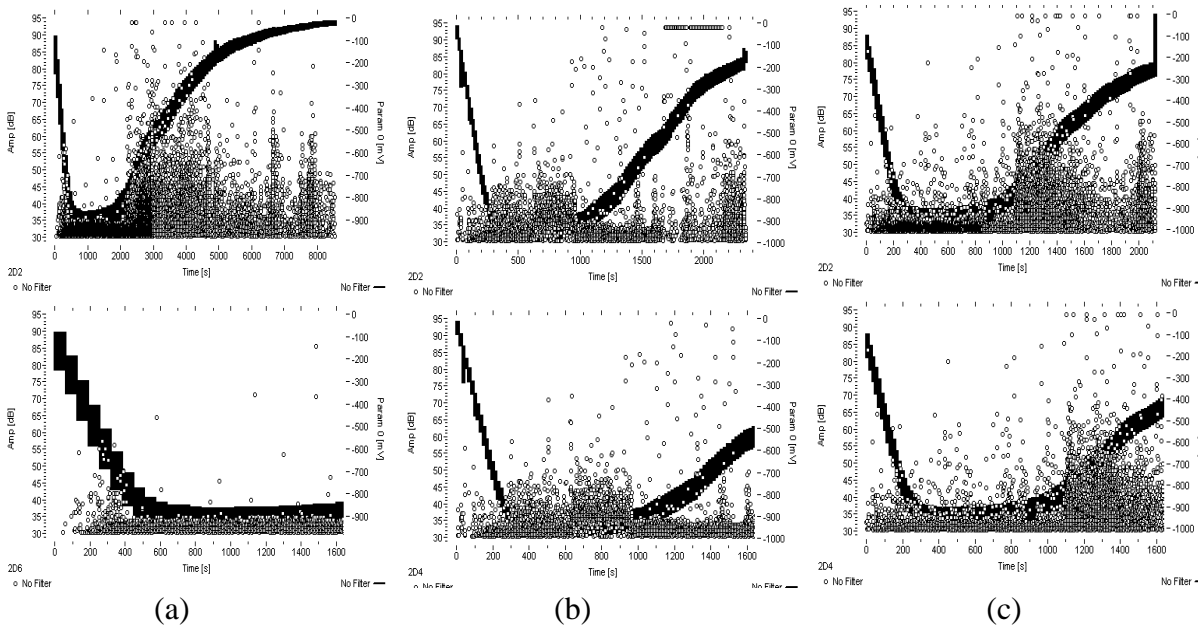
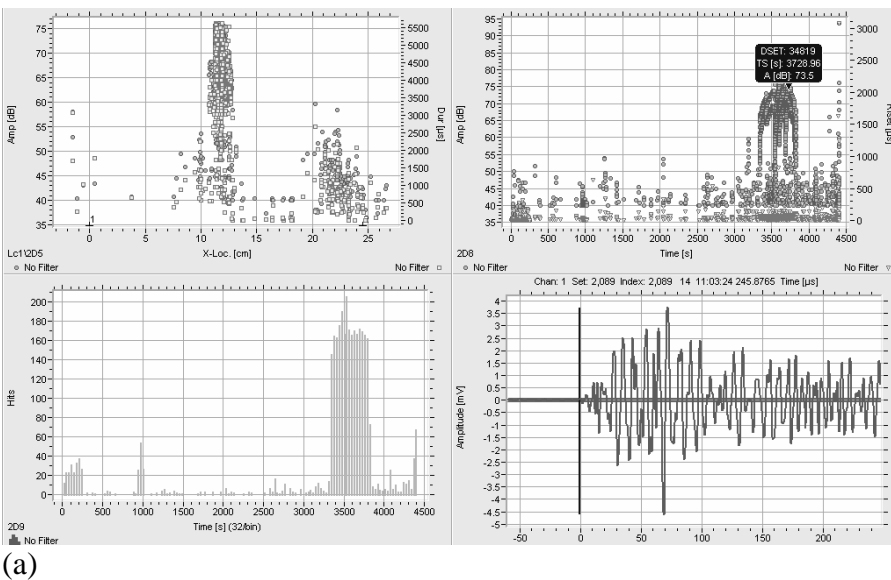
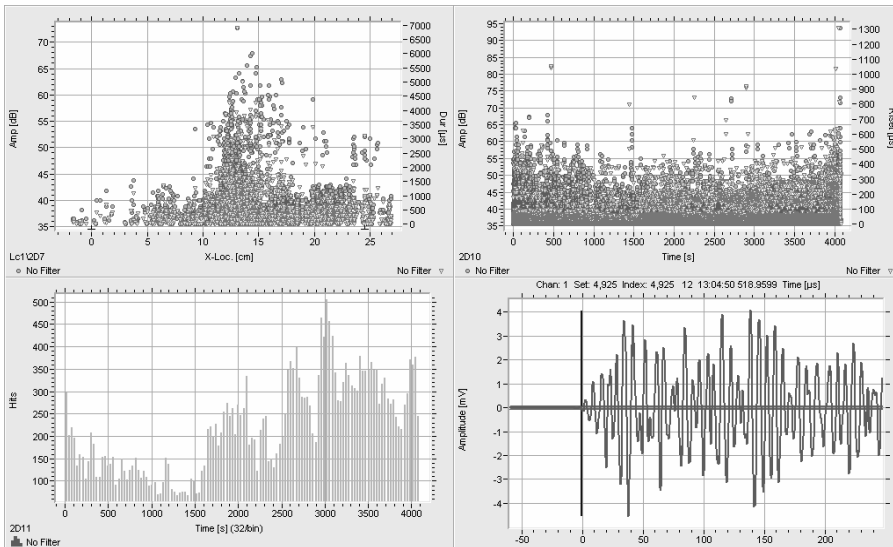


Figure (7) Flexural test on Al sample: amplitude ~ load vs time, [>1600 s, 1600s] plots a. Reference b. Marine c. humid

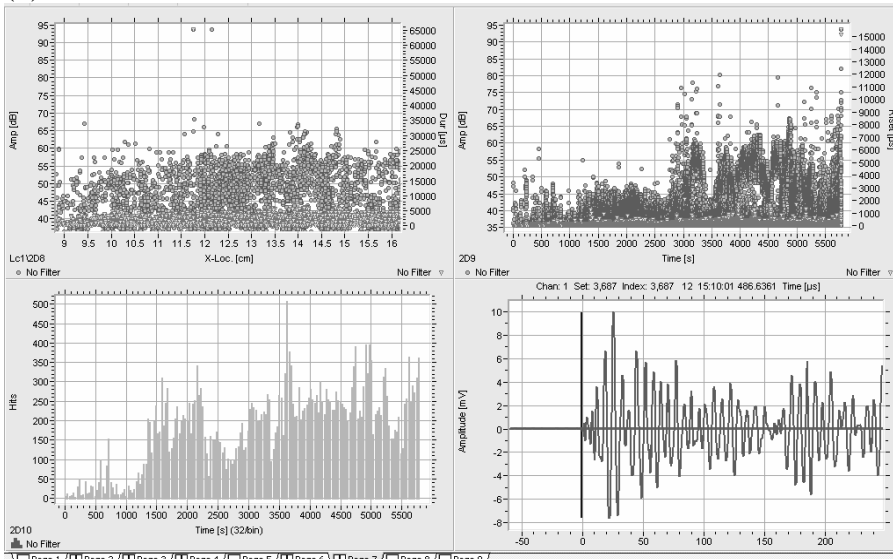
Figure (8) Top row: peak amplitude ~ duration versus location, peak amplitude ~ rise time versus time. Bottom row: hits versus time and signal waveform. a. Reference. b. Marine c. Humid



(a)



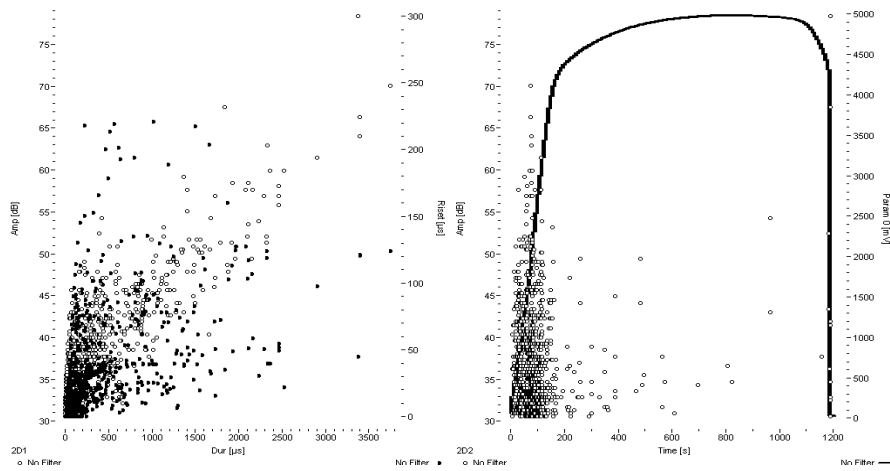
(b)



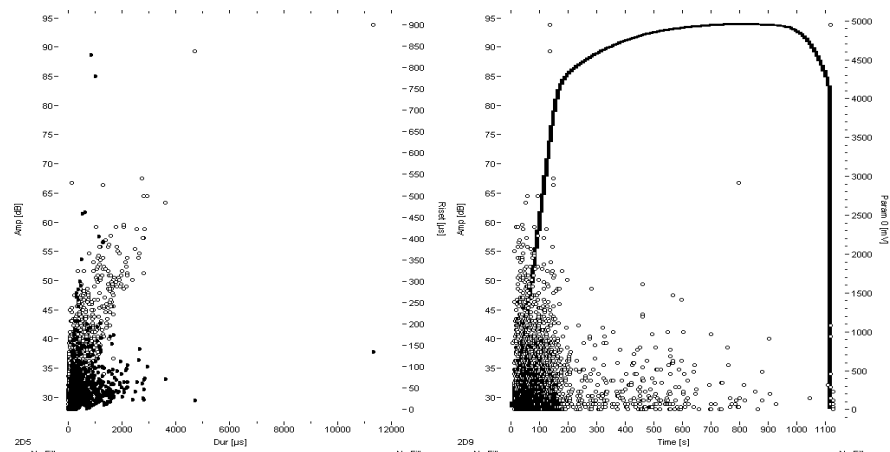
Page 1 Page 2 Page 3 Page 4 Page 5 Page 6 Page 7 Page 8 Page 9

(c)

(a)



(b)



(c)

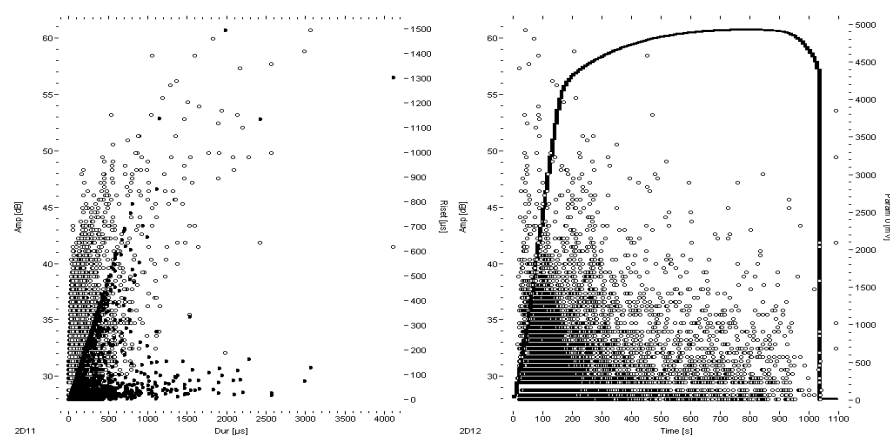


Figure (9) Tensile test: (a) Reference sample, (ncal), (b) Corroded humid, (hcal) (c) Corroded Marine, (mcal)

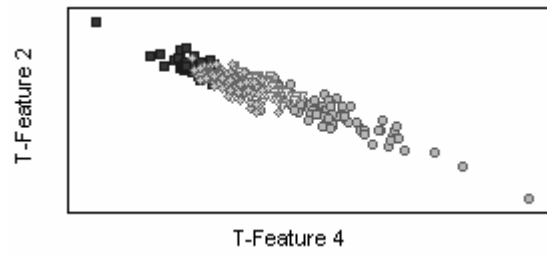


Figure (10a) Unsupervised classification on corroded (humid) aluminium sample (alhc)

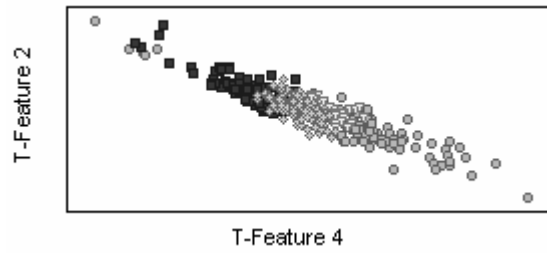


Figure (10b). Unsupervised classification alhc applied to marine corroded sample almc

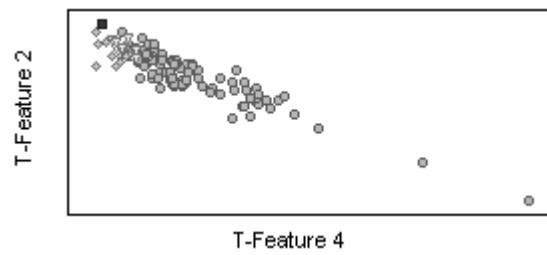
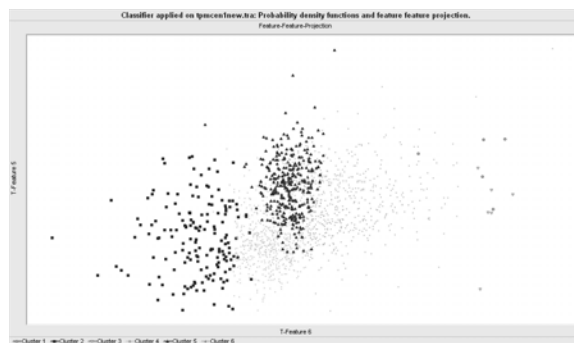
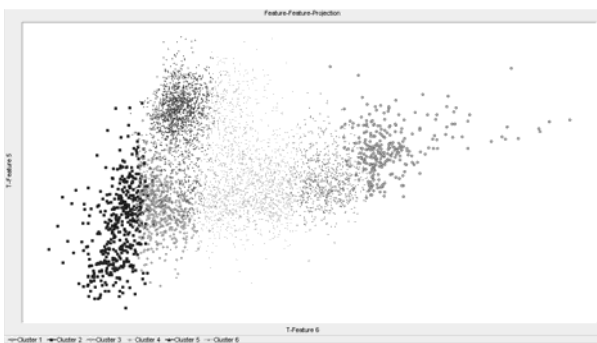


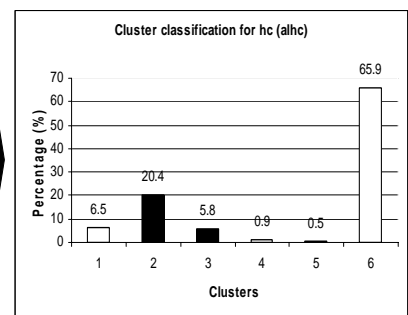
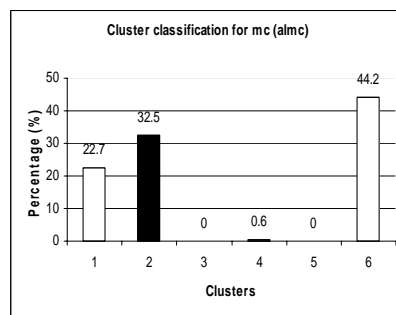
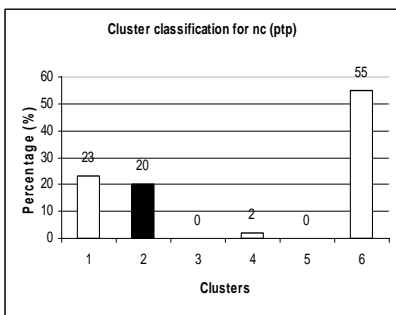
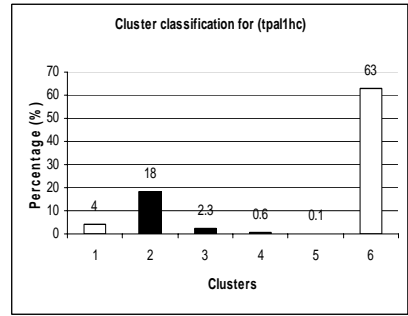
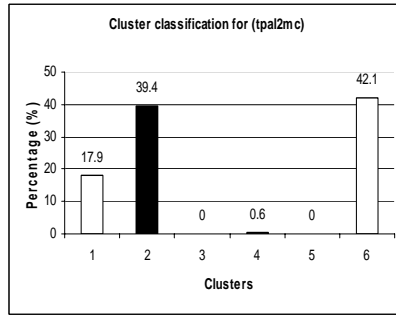
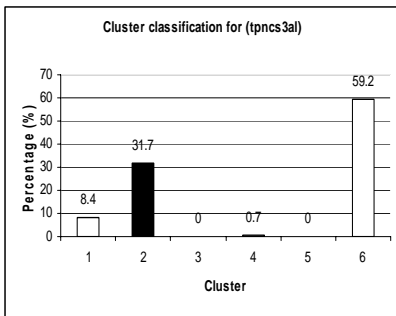
Figure (10c). Unsupervised classification alhc applied to reference sample alnc

Figure (11a)

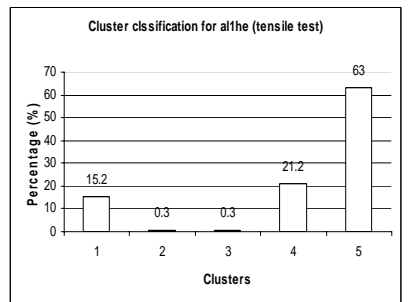
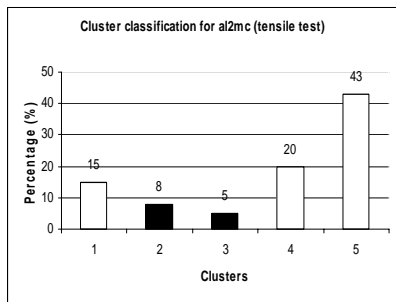
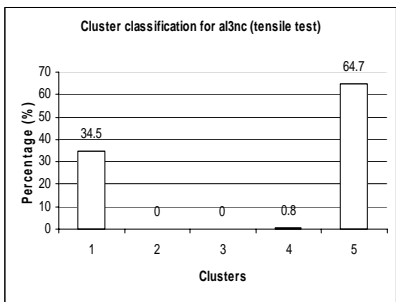
Figure (11b)



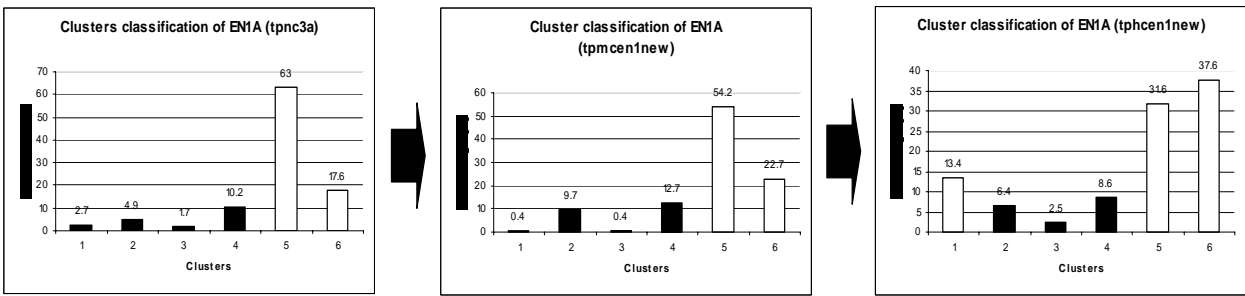
Aluminium (original data)



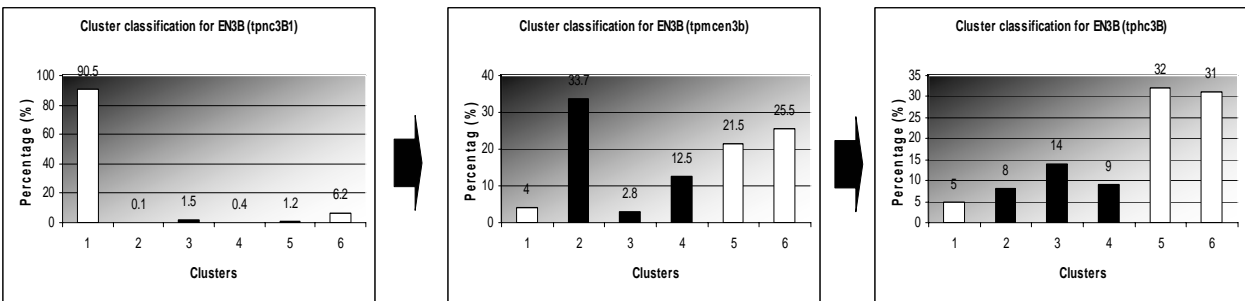
Tensile test for Aluminium



EN1A



EN3B



Aluminium

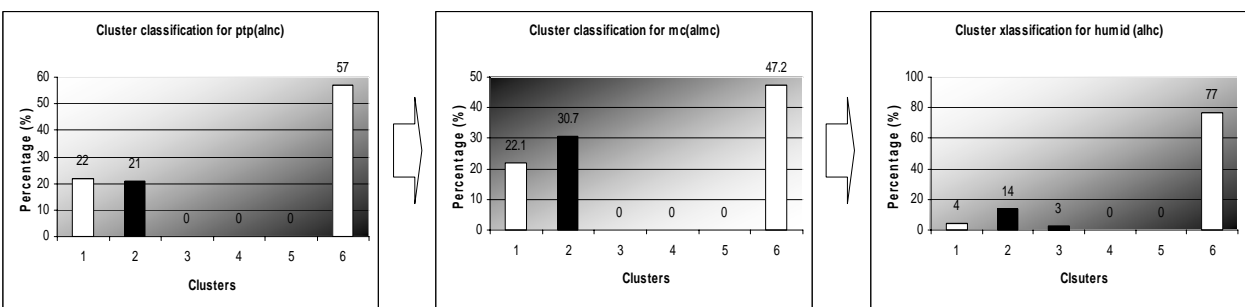


Figure 12

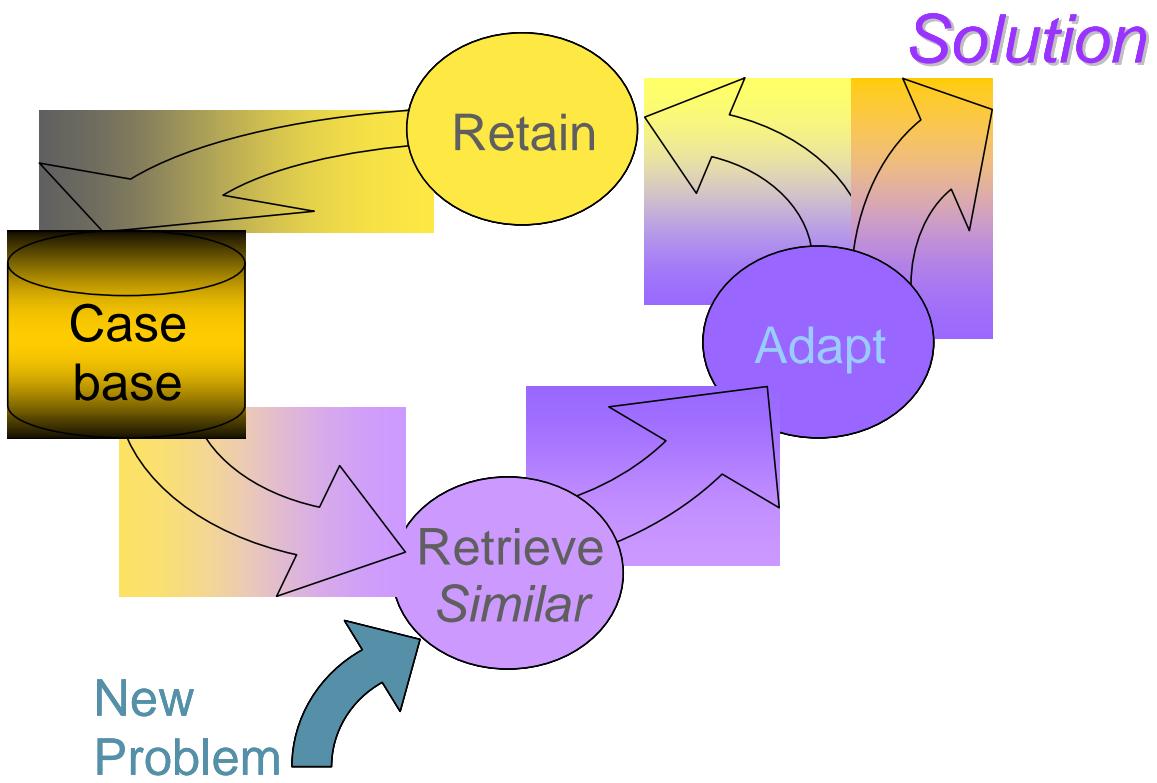


Figure (13)